Jurnal Fisika Flux: Jurnal Ilmiah Fisika FMIPA Universitas Lambung Mangkurat
Volume 23, Issue 2, August 2026
1819-796X (p-ISSN); 2541-1713 (e-ISSN)
https://ppjp.ulm.ac.id/journal/index.php/f *Research Article*

Uncertainty Analysis of 1D Magnetotelluric Inversion Model Using the Neighborhood Algorithm: Application to Kilauea Volcano

Anwar Udin Sayfulloh[1)], Andri Yadi Paembonan[1)], Wahyu Eko Junian[1,*)]
Study Program of Geophysical Engineering, Faculty of Industrial Technology,
Institut Teknologi Sumatera

Correspondence email: wahyu.junian@tg.itera.ac.id

DOI: https://doi.org/10.20527/flux.v23i2.25876

Received: 13 April 2026; Revised: 3 May 2026; Accepted: 4 May 2026

ABSTRACT

Magnetotellurics (MT) is a passive geophysical method that relies on the principles of electromagnetic induction to delineate subsurface resistivity distributions. This study implements the Neighborhood Algorithm (NA) for one-dimensional (1D) inversion of MT data to overcome local minima traps and analysis model uncertainty. The performance of the NA is evaluated using the Rosenbrock function and synthetic MT data. The evaluation results show that the NA successfully achieves convergence with a misfit of less than 2.0 on synthetic data with 5% added Gaussian noise. Furthermore, the NA is applied to field MT data from Kilauea Volcano, Hawaii. The performance of the NA in modeling the field data is compared to a conventional approach, namely the Levenberg-Marquardt (LM) algorithm. The field data modeling results demonstrate that the NA (misfit 1.99) outperforms the LM algorithm (misfit 2.52). Additionally, the NA provides supplementary information in the form of a posterior probability density that maps the model's uncertainty bounds. The resistivity model, supported by uncertainty analysis, strengthens the information at Kilauea Volcano regarding the presence of a low-resistivity (conductive) zone at a depth of less than 3 km, which is associated with a shallow magma chamber (partial melt) or saline fluids.
KEYWORDS : Uncertainty analysis; inversion; magnetotelluric; neighborhood algorithm

INTRODUCTION

The magnetotelluric (MT) method is a geophysical method capable of imaging the subsurface resistivity distribution by measuring time-varying electromagnetic fields (electric field $\boldsymbol{E}$ and magnetic field $\boldsymbol{H}$) at the surface (Cagniard, 1953). The use of low frequencies in this method allows for a very deep investigation penetration, although it requires a longer recording duration due to the low amplitude of natural magnetic signals (Telford et al., 1990). The MT method has been widely applied in various studies, such as global tectonic studies to identify geological structures and active fault zones (Unsworth et al., 2005; Ingham & Brown, 1998; Sun et al., 2020). In addition, the MT method is also widely applied in the early stages of geothermal exploration to map the clay cap and reservoir system (Ladanivskyy et al., 2021; Simeng et al., 2025; Mekkawi et al., 2022; Patro, 2017).

In regions with relatively simple and laterally homogeneous geological conditions, one-dimensional (1D) modeling is often considered sufficiently representative to depict vertical resistivity variations (Junian et al., 2025; Junian et al., 2026). In general, conventional MT inversion modeling relies on linearization approaches such as the Occam inversion (Ariani & Srigutomo, 2016) dan *Levenberg-Marquardt* (LM) (Darisma & Marwan, 2019). However, this approach highly depends on the initial model and is prone to getting trapped in local minima due to the highly non-linear nature of the relationships between subsurface parameters. In addition, MT inversion results are often non-unique due to equivalence problems, such as the emergence of model solutions in the form of very thin conductive layers that are physically irrelevant to the actual geological conditions (Ekaputri et al., 2018).

To overcome these limitations, various global approach algorithms have been widely used in inversion modeling. Metaheuristic algorithms based on Particle Swarm Optimization (PSO) offer a better global solution search (Cui et al., 2020; Junian et al., 2023; Pace et al., 2019). On the other hand, modern approaches based on deep learning (Khatami & Grandis, 2023; Saibi et al., 2026) as well as advanced probabilistic model evaluations such as Normalizing Flows (NF) (Wu et al., 2025) and Invertible Neural Networks (INN) (Bittar et al., 2026) have proven effective for use in geophysical modeling. Nevertheless, the implementation of deep learning requires complex architectures and highly depends on the quantity and quality of the training data.

As an efficient and stable alternative for 1D modeling with a relatively small number of parameters, this study implements a global optimization inversion approach using the Neighborhood Algorithm (NA) (Sambridge, 1999a). The main advantage of NA lies in its low parameter setup redundancy compared to other stochastic algorithms, making it more consistent without the need for complex variable tuning. Instead of searching for a single model only, the NA Appraise framework (Sambridge, 1999b) is capable of evaluating a collection of models to generate the Posterior Probability Density (PPD) through Voronoi cell interpolation without conducting additional forward modeling. This approach allows model uncertainty to be achieved with precision, producing a more robust interpretation, as well as providing confidence level information regarding the range of solutions (Yoshizawa & Kennett, 2002; Ojo et al., 2017; Yao, 2015).

To test the reliability of this algorithm, this study will implement NA on synthetic MT data before applying it to field data from Kilauea Volcano, Hawaii, acquired during the 2002–2003 period (prior to the major 2018 eruption phase). Kilauea is a highly active volcanic system, dominated by seismic activity, main rift zones, and a central magma reservoir (Hoversten et al., 2022). Therefore, the MT method becomes crucial for directly imaging the distribution of magma melt based on its resistivity contrast. The performance of the NA algorithm in this study will be directly compared with the conventional LM algorithm to demonstrate its advantages in overcoming local minima traps and mapping low-resistivity zones associated with shallow magma pockets more convincingly.

METHODS

Forward Modeling

The MT impedance (Z) is defined as the ratio between the horizontal electric field component E and the horizontal magnetic field component H, which is mathematically expressed as:

$$Z_{xy} = \frac{E_x}{H_y} \; and \; Z_{yx} = \frac{E_y}{H_x} \quad (1)$$

In one-dimensional (1D) modeling the diagonal elements of the impedance tensor are zero ($Z_{xx} = Z_{yy} = 0$) and the off-diagonal elements satisfy ($Z_{xy} = -Z_{yx}$), the earth is assumed to be composed of horizontally layered strata that are laterally homogeneous, where each layer is characterized by a specific resistivity and thickness value, while the last layer is considered a half-space. This allows the impedance calculation to be performed recursively from the deepest layer toward the top layer (Grandis, 1999). The recursive formulation provides a framework for simulating the magnetotelluric response of layered media over a wide range of frequencies. The resulting impedance values can subsequently be used to derive apparent resistivity and phase responses.

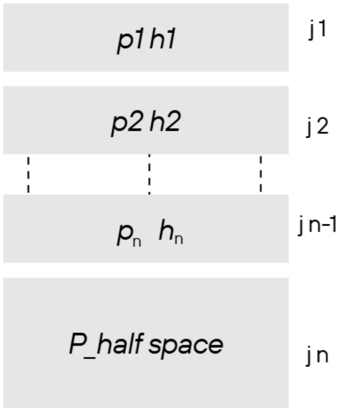

Figure 1. Vertically layered earth model

For each j-th layer Figure 1, the induction parameter coefficient is defined as:

$$\gamma_j = \sqrt{i\omega\mu_0\sigma_j} \quad (2)$$

Where ω is the angular frequency, μ_0 is the vacuum permeability and σ is the conductivity of the j-th layer, then the intrinsic impedance of the layer is expressed as:

$$w_j = \gamma_j \rho_j \quad (3)$$

The resistivity of the j-th layer or ρ_j and γ_j represents the j-th induction parameter coefficient. The measured surface impedance or total impedance at the upper boundary of the j-th layer is calculated using the following recursive relationship:

$$Z_j = w_j \frac{1 - R_j e^{-2\gamma_j h_j}}{1 + R_j e^{-2\gamma_j h_j}} \quad (4)$$

with the electromagnetic reflection coefficient R between layers given by:

$$R_j = \frac{w_j - Z_{j+1}}{w_j + Z_{j+1}} \quad (5)$$

where h_j is the thickness of the j-th, and Z_{j+1} represents the impedance of the layer beneath it. For the last layer (basement), the impedance is assumed to be equal to the intrinsic impedance of the half-space. Based on the surface impedance Z_1, the MT response can then be expressed in the form of apparent resistivity ρ_a and phase φ.

$$\rho_a = \frac{1}{\omega\mu_0}|Z_1|^2 \quad (6)$$

$$\varphi = tan^{-1}\left(\frac{Im(Z_1)}{Re(Z_1)}\right) \quad (7)$$

NA Search Stage

The Neighborhood Algorithm (NA) is a directed stochastic search method similar to the Genetic Algorithm (GA) and Simulated Annealing (SA), which guides parameter space sampling based on previous results so that unpromising areas are rarely sampled, by balancing exploitation and exploration to find the global minimum or the best solution (Wathelet, 2008).

The determination of the Voronoi cell boundaries is performed for each parameter i using Gibbs sampling. The boundary intersection point or X_{ji} between the Voronoi cell of the central model v_k and another model v_j in the i-th dimension is calculated using:

$$x_{ji} = \frac{1}{2}\left[v_{ki} + v_{ji} + \frac{d_k^2 - d_j^2}{v_{ki} - v_{ji}}\right] \quad (8)$$

v_{ki} is the parameter value of the central model k on the i-th axis and v_{ji} is the parameter value of the neighboring model j within the ensemble on the i-th search axis, while d_k^2 and d_j^2 are the squared perpendicular distances of the central model k and neighboring model j from their respective models to that axis. Within the lower and upper boundary space of the Voronoi cell in the i-th dimension, *with* X_{Ai} as the i-th parameter value of the central model, it is determined as (Sambridge, 1999a):

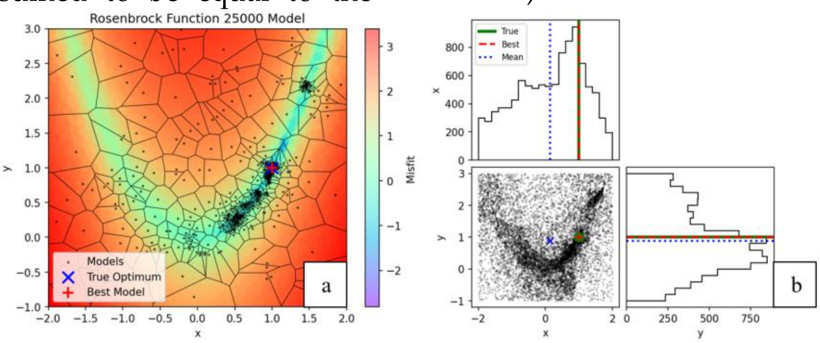

Figure 2. Objective Function *Rosenbrock 2D* (a) NA *Searcher* and (b) NA *Appraise*

https://doi.org/10.20527/flux.v23i2.25876

$$lb = \max[l_i, x_{ji}] \text{ for } x_{ji} \leq x_{Ai} \quad (9)$$

$$ub = \min[u_i, x_{ji}] \text{ for } x_{ji} \geq x_{Ai} \quad (10)$$

After random sampling of X_{Bi} is performed at the boundaries *lb* and *ub*, the perpendicular distance of each model to the parameter axis is then recursively updated as the random walk moves to the next dimension. Figure 2 (a) illustrates the implementation of this algorithm in solving an optimization problem in a 2D space, defined as the Rosenbrock objective function (Ma & Li, 2019). This approach avoids recalculating the distance across all dimensions, thereby reducing the computational cost to a linear scale.

$$\left(d_j^2\right)_{i+1} = \left(d_j^2\right)_i + \left(v_{ji} - x_{Bi}\right)^2 - \left(v_{ji+1} - x_{Bi+1}\right)^2 \quad (11)$$

NA Appraisal Stage

The next stage is the appraisal phase, which is the process of statistical evaluation and interpretation of the entire collection of models generated during the search process. Information from all models is utilized to construct an approximation of the posterior probability density (PPD) function by leveraging the Voronoi cell geometry approach without conducting forward modeling. The tail areas of this distribution represent models with high misfit, while the width or variance of the distribution serves as a quantitative measure of the uncertainty of the modeled parameters (Bodin et al., 2012). To generate new samples whose distribution matches the shape of the approximate PPD (P_{NA}), a rejection method is applied. A random number *r* within the range (0,1) is generated to test the candidate. The random walk step will be accepted, and the model position shifts to X_{pi} if it satisfies the condition (Sambridge, 1999b).

$$\ln(r) \leq \ln\left(P_{NA}\left(X_{pi} \middle| X_{-i}\right)\right) - \ln(P_{max}) \quad (12)$$

$\ln(P_{NA}\ (X_{pi}\ /\ X_{-i}\ ))$ is the log-probability value at the Voronoi cell where the candidate X_{pi} is located, and $\ln(P_{max})$ is the highest log-probability value along that search axis. In Figure 2(b), it can be seen that a very good ensemble of new samples is generated, distributed following the high probability of the Rosenbrock objective function.

Optimization and Parameter Tuning

The performance of the NA algorithm was tested using synthetic 1D MT data generated from a homogeneous half-space model (Model 1) with a resistivity ρ value of 1000 *Ohm.m* and a 4-layer model (Model 2) with resistivity parameters of ρ_1 = 50 *Ohm.m*, ρ_2 = 500 *Ohm.m*, ρ_3 = 10 *Ohm.m* dan ρ_4 = 1000 *Ohm.m* dengan ketebalan h_1 = 200 meter, h_2 = 500 meter dan h_3 = 800 meter. A 5% Gaussian noise was added to the synthetic data to simulate field data that is frequently corrupted by noise.

Code optimization was performed using the Numba JIT (Just-In-Time) library with Python version 3.13.7. The selection of Numba was based on its capability to transform Python code into machine instructions equivalent to low-level languages such as C (Stoico et al., 2025). In the testing conducted, using the Numba JIT compiler successfully reduced the forward modeling time for one million 3-layer configuration models (5 model parameters) from 4 minutes 39 seconds to just 5 seconds, which translates to 55,8 times faster.

The inversion parameters used for this test are an initial model size (n_i) of 1,500, new samples generated per iteration (n_s) of 150 and the number of best Voronoi cells (n_r) set to 10 to keep the algorithm exploratory in low-misfit areas without getting trapped in local minima. The search is limited to 500 iterations (n_{iter}) to achieve a stable convergence condition, this configuration produces a total ensemble of 76,350 models with an execution time of approximately 12 seconds for a 3-layer model. The parameter exploration space is bounded within a resistivity range of 1 to 2,000 *Ohm.m* and a thickness range of 1 to 1,100 *meter* referring to the prior literature on the target depth to be inverted (Hoversten et al., 2022). This configuration can yield an effective model depth value of approximately 4,4 km.

The search ensemble was downsampled by 50% to reduce excessive computational burden for evaluation during the appraisal phase to generate 10,000 new probability samples. The robustness of the algorithm was tested using field data through a comparison with the conventional Levenberg-Marquardt (LM) method. This comparative inversion utilizes a 4-layer configuration with absolute free parameters and is executed for 50 iterations with a damping value (λ) of 0,1 and a perturbation factor of 0,1%. The inverted data consists of the determinant invariant magnetotelluric impedance tensor from the Saddle measurement station in the Kilauea Volcano area, Hawaii (Hoversten & Gasperikova, 2022). The misfit function used to measure the degree of agreement between the observed data and the forward modeling model responses is defined as follows (Syaripudin & Grandis, 2001):

$$misfit = \sum_{i=1}^{N} \left(\begin{array}{c} \left| log_{10} \left(\frac{\rho_{Obs,i}}{\rho_{fwd,i}} \right) \right| + \\ \lambda \left| \left(\phi_{obs,i} - \phi_{fwd,i} \right) \right| \end{array} \right) \quad (13)$$

$\rho_{Obs,i}$ as the observed resistivity and $\rho_{fwd,i}$ the calculated resistivity, with $\lambda = 1$ is the weighting factor for phase relative to apparent resistivity data, $\phi_{obs,i}$ the observed phase and $\phi_{fwd,i}$ as the calculated phase.

The general workflow of the NA search and appraisal algorithm in this study can be observed in two stages. The search stage (NA_I) exploring the multidimensional parameter space using Voronoi cell geometry. It begins by generating n_i random models and selecting n_r models with the lowest misfit values. For each parameter axis, the Voronoi intersection points are calculated using perpendicular distances to define localized search boundaries. Candidate samples are then randomly generated within these upper and lower bounds, after which the perpendicular distances is continuously updated.

The appraisal stage (NA_II) quantifies parameter uncertainties by applying misfit values are first converted into log-posterior probabilities, and a random walk is initialized from an ensemble model. Sequentially along each parameter axis, the algorithm computes Voronoi intersection points, generates a candidate sample Xp_i, identifies its enclosing Voronoi cell, and evaluates it using a acceptance/rejection rule. This Gibbs sampling process repeats for n resamples iterations to construct the posterior distribution.

RESULTS AND DISCUSSION

This section presents the performance evaluation results of the Neighborhood Algorithm (NA), starting with testing on synthetic data before its application to the Kīlauea Volcano field data. The synthetic tests are used to assess the accuracy and reliability of the algorithm, while the field-data application demonstrates its effectiveness under real geological conditions.

The approach in Figure 3(a) which achieves a misfit of 1.65 is designed to evaluate the robustness of the appraisal phase in handling parameter ambiguity issues. The most crucial finding from this test, shown in Figure 4(a) is observed in the posterior distributions for the thickness parameters h_1 and h_2. The probability density functions for both parameters are widely distributed from 0 to 1,100 meters and have many solutions, indicating a lack of specific resolution at any single depth. This behavior indicates that multiple combinations of layer thicknesses can produce similar magnetotelluric responses, resulting in a non-unique solution. Consequently, the appraisal stage assigns comparable probabilities to a broad range of thickness values, reflecting the uncertainty associated with resolving layer boundaries.

https://doi.org/10.20527/flux.v23i2.25876

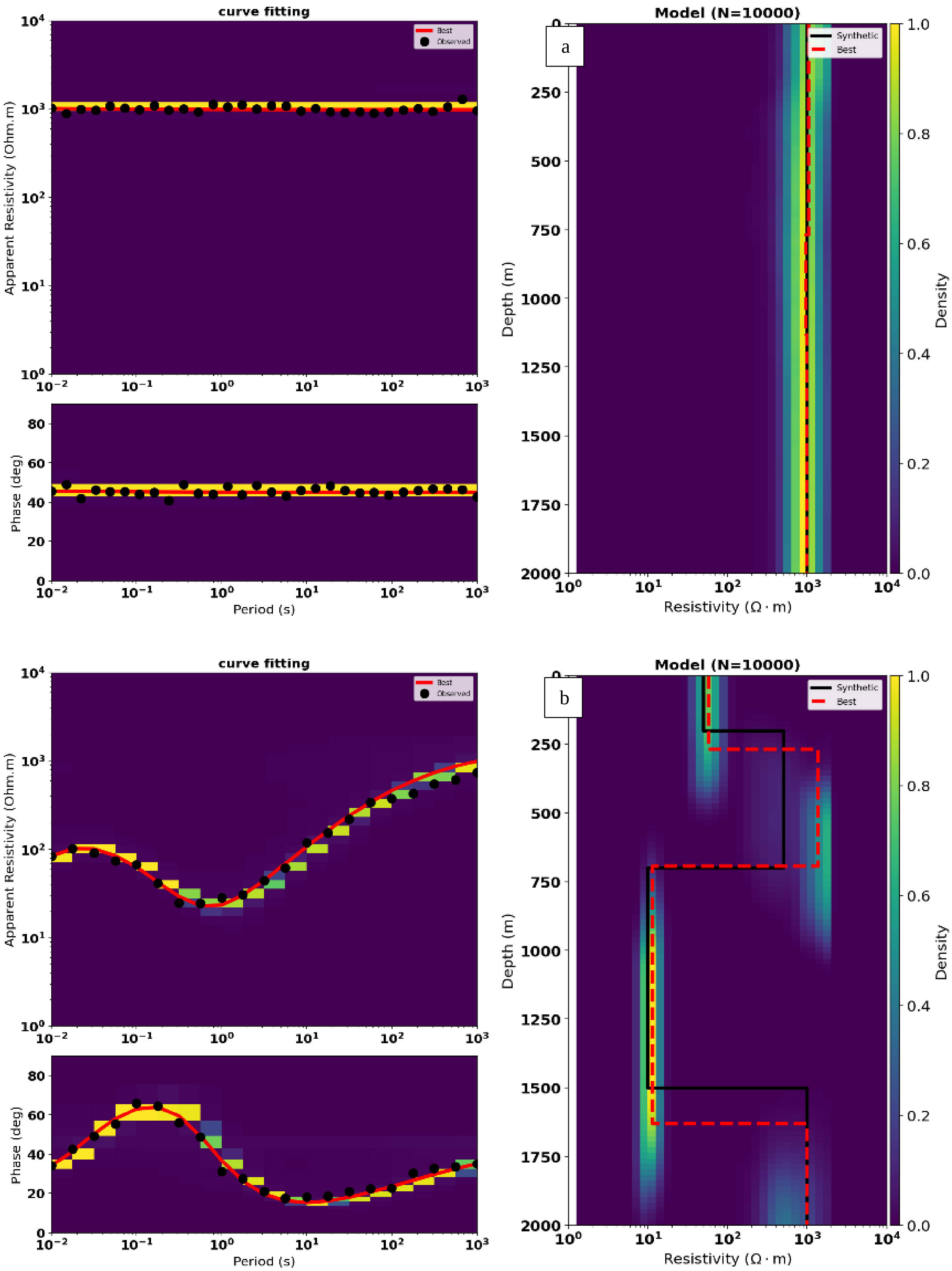

Figure 3 From synthetic testing with posterior model density, the best misfit obtained was 1.65 for (a) Model 1 and 1.18 for (b) Model 2

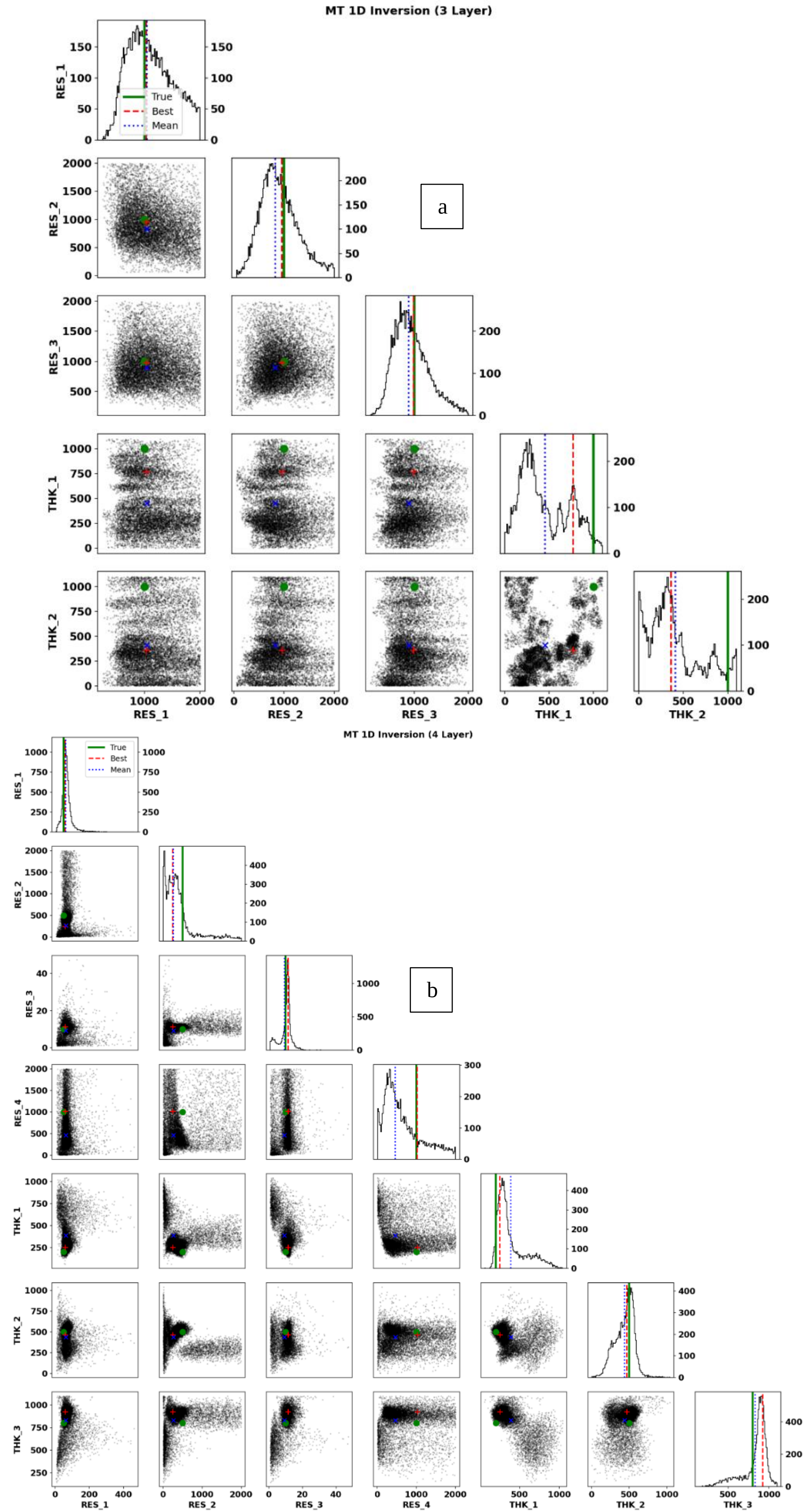

Figure 4. Corner plot of the appraisal phase for (a) Model 1 and (b) Model 2. The green lines and dots represent the synthetic model, the red color indicates the best model, the blue color represents the average model and the y-axis of the histogram is the frequency of the data

The more complex four-layer synthetic earth model forms a K-H type anomaly pattern, as shown in Figure 3(b). This pattern is characterized by a low-high-low resistivity sequence (K-type) followed by a high-low-high sequence (H-type). The inversion results demonstrate the achievement of a highly stable global minimum misfit convergence of 1.18, evidenced by the precise agreement of the data response curves across the entire period spectrum. The parameter space evaluation in Figure 4(b) successfully maps the equivalence phenomenon in the resistive second layer of 500 *Ohm.m*. Given that induced magnetotelluric currents have low sensitivity to resistive zones sandwiched between conductive zones, the algorithm objectively represents this data limitation through a widening of the posterior probability distribution (PPD) for the ρ_2 and ρ_4 parameters, while simultaneously performing parameter compensation with a bimodal distribution to achieve model fitting.

As a final proof of concept, the algorithm was applied to field data consisting of the invariant magnetotelluric impedance tensor from a measurement site at Kīlauea Volcano, Hawaii. The limitations of this study include the 1D assumption, under these conditions spatial distortion phenomena can arise, if in other data cases there are conductive features adjacent to the measurement station may be vertically projected and interpreted as subsurface layers (such as a pseudo-layer).

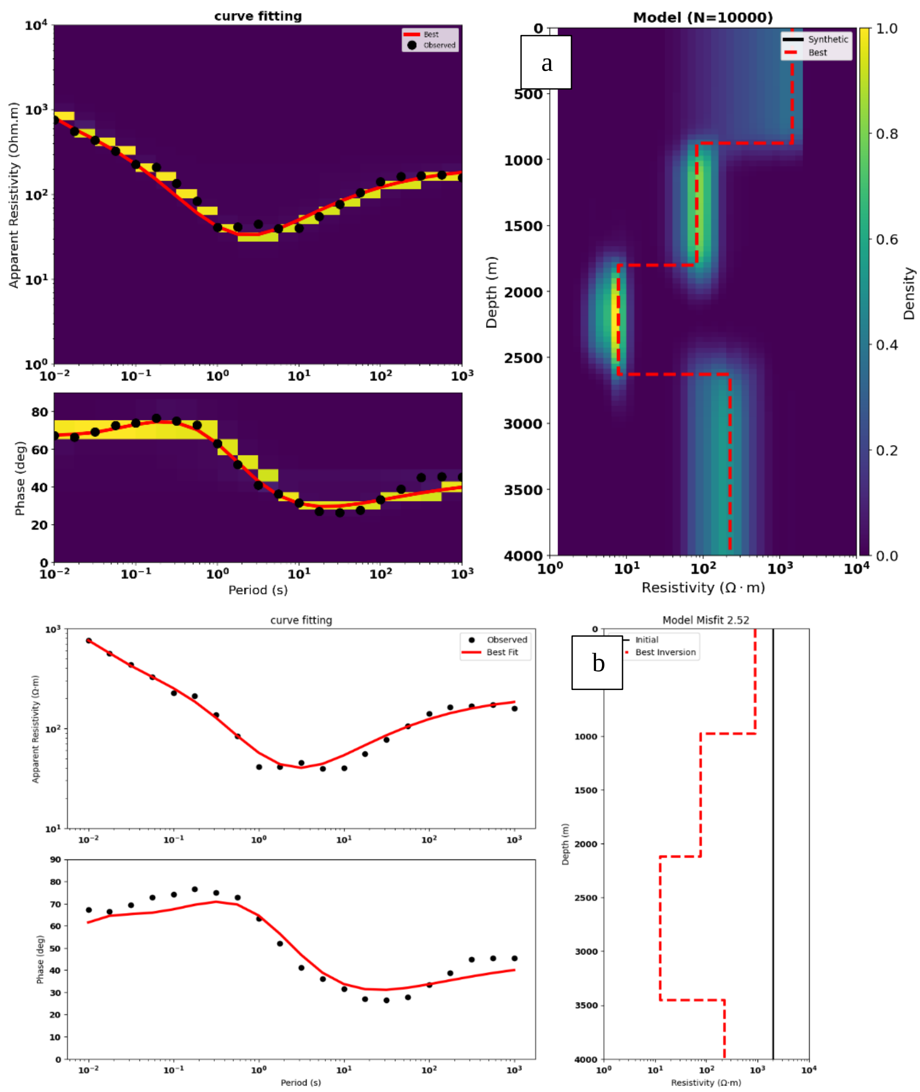

Figure 5. Data fitting curves for field data testing, with the best misfit obtained being (a) 1.99 for NA with posterior model density and (b) 2.52 for Levenberg-Marquardt (LM)

However, the application to this field data is primarily focused on validating and analysis model uncertainty in 1D magnetotelluric data inversion, while simultaneously comparing the performance of the NA search algorithm with the conventional gradient-based deterministic LM inversion method. In the NA method, Figure 5(a) demonstrates a significantly better optimization performance compared to the LM method shown in Figure 5(b). This is evidenced by the achievement of a lower minimum misfit value of 1.99 for the NA algorithm, compared to 2.52 for the LM algorithm. The primary advantage of the NA algorithm lies in its capability to provide uncertainty information through the appraisal phase. Based on previous geophysical studies in the Kīlauea region, the subsurface structure is dominated by the presence of a highly conductive anomalous zone of 2–3 *Ohm.m* at shallow to intermediate depths of less than 3 km, which correlates with the presence of a shallow magma chamber (partial melt) or saline fluids within the hydrothermal system (Hoversten et al., 2022). In the 1D profile resulting from the NA inversion in Figure 5(a), the presence of this conductive layer was successfully reconstructed with high fidelity.

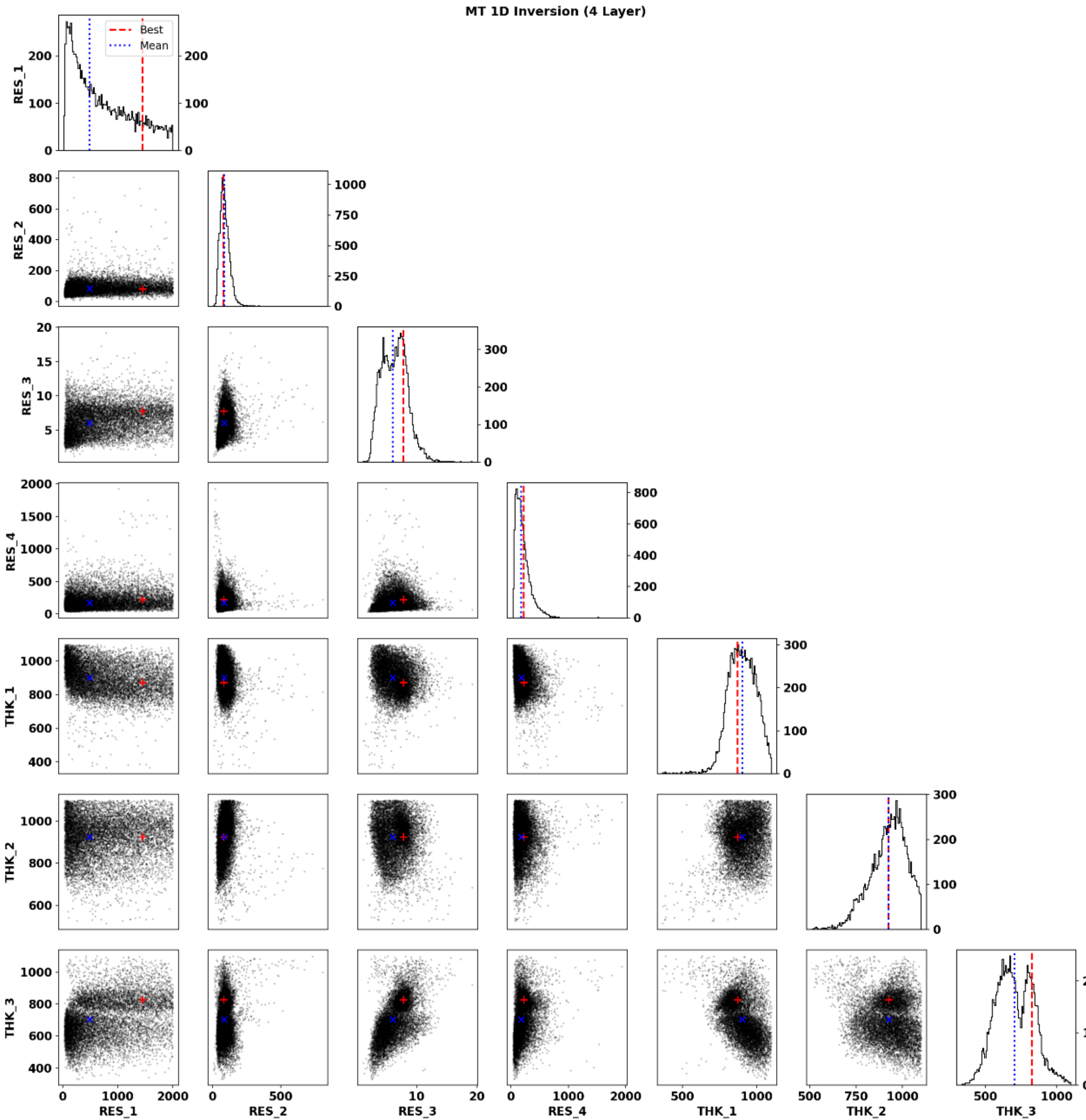

Figure 6. Corner plot of the appraisal phase from the field data model ensemble. The red lines and dots represent the best model, while the blue color indicates the average model.

The contrast to the LM method shown in Figure 5(b), which only presents a single model that implies absolute certainty, the NA algorithm probabilistically detects and maps the resolution level of the volcanic anomaly. The posterior probability density (PPD) function transparently exhibits the uncertainty distribution of both the resistivity and layer thickness parameters. This resolution limit is due to the conductive shielding effect of the overlying magmatic/hydrothermal fluids, as well as signal attenuation caused by environmental noise, which leads to a loss of sensitivity in the objective function toward specific layer parameters. This creates a broad solution space topography where multiple parameter combinations can yield identical model responses. Consequently, the appraisal phase maps this region as a zone characterized by low-confidence probability.

The model evaluation shown in Figure 6 the highest resolution is consistently observed in the third-layer resistivity parameter ρ_3 which sharply narrows down to a highly conductive anomaly of less than 10 *Ohm.m*, physically validating the presence of a shallow magma chamber or hydrothermal fluids at a depth of less than 3 km, in agreement with the literature by (Hoversten et al., 2022). The Gaussian distribution of the parameters that tends to be narrow and sharp indicates high resolution. On the other hand, the widened probability distribution for parameter ρ_1 due to sensitivity of the resistive rock contact at the surface, ρ_4 represents the low sensitivity of the deep resistive layer. The results of this field data testing have a very good suitability with a fairly strict resolution range that can be trusted.

CONCLUSION

This study successfully demonstrated the effectiveness of the Neighborhood Algorithm (NA) optimized using the Numba JIT compiler, achieving a computational speedup of up to 55.8 times in three-layer forward modeling for the evaluation of one million models. Testing using synthetic data with 5% Gaussian noise added showed excellent algorithm performance, with misfit values of 1.65 for Model 1 and 1.18 for Model 2. In the application to field data from Kīlauea Volcano, the NA algorithm demonstrated its good by producing a misfit of 1.99, which is lower and more accurate than that obtained using the conventional Levenberg–Marquardt method 2.52.

The NA modeling results also convincingly identified a conductive anomaly zone at depths shallower than 3 km, associated with a hydrothermal system or a shallow magma chamber, consistent with the understanding of the volcanic geological structure in the area. Furthermore, the appraisal stage confirmed the capability of NA to reconstruct the model and qualitatively resolve uncertainty probabilities very well. Overall, these results indicate that the NA approach demonstrates strong robustness under the tested conditions.

ACKNOWLEDGMENTS

We would like to express our sincere appreciation and gratitude to Auggie Marignier (Department of Earth Sciences, University of Oxford) for his open-source code contribution, which served as the technical foundation and inspiration for the algorithm development in this study. We also extend our gratitude to Hoversten, G., and Gasperikova, E., as well as the Geothermal Data Repository (GDR) of Lawrence Berkeley National Laboratory for providing the Kīlauea Magnetotelluric Dataset.

REFERENCES

Ariani, E., & Srigutomo, W. (2016). 1D and 2D Occam's inversion of magnetotelluric data applied in volcano-geothermal area in Central Java, Indonesia. *Journal of Physics: Conference Series, 739*, 012036. https://doi.org/10.1088/1742-6596/739/1/012036

Bittar, G., Wu, S., Su, Y., Zeng, S., Sun, J., Wu, X., Huang, Y., & Chen, J. (2026). Invertible neural network for real-time inversion and uncertainty quantification of ultra-deep resistivity measurements. *Computers & Geosciences, 207*, 106067. https://doi.org/10.1016/j.cageo.2025.106067

Bodin, T., Sambridge, M., Tkalčić, H., Arroucau, P., Gallagher, K., & Rawlinson, N. (2012). Transdimensional inversion of receiver functions and surface wave dispersion. *Journal of Geophysical Research: Solid Earth,* *117*(B2),B02301.https://doi.org/10.1029/2011JB008560

Cagniard, L. (1953). Basic theory of the magneto-telluric method of geophysical prospecting. *Geophysics,18*(3),605-635. https://doi.org/10.1190/1.1437915

Cui, Y., Zhang, L., Zhu, X., Liu, J., & Guo, Z. (2020). Inversion for magnetotelluric data using the particle swarm optimization and regularized least squares. *Journal of Applied Geophysics,181*,104156.https://doi.org/10.1016/j.jappgeo.2020.104156

Darisma, D., & Marwan. (2019). One-dimensional magnetotelluric inversion using Levenberg-Marquardt and particle swarm optimization algorithm. *IOP Conference Series: Earth and EnvironmentalScience,364*,012035.https://doi.org/10.1088/1755-1315/364/ 1/012035

Ekaputri, D., Maulinadya, S., & Grandis, H. (2018). Simple equivalence analysis for magnetotelluric (MT) depth resolution in layered earth model. *The 43rd Annual Scientific Meeting Himpunan Ahli Geofisika Indonesia.* library.hagi.or.id/wp-content/uploads/2025/01/PITHAGI2018-101.pdf

Grandis, H. (1999). An alternative algorithm for one-dimensional magnetotelluric response calculation. *Computers & Geosciences, 25*(2), 119-125. https://doi.org/ 10.1016/S0098-3004(98)00110-1

Hoversten, G. M., & Gasperikova, E. (2022). Kilauea Magnetotelluric Dataset. [Data set]. Geothermal Data Repository. *Lawrence Berkeley National Laboratory*. https://doi.org/10.15121/1872965

Hoversten, G. M., Gasperikova, E., Mackie, R., Myer, D., Kauahikaua, J., Newman, G. A., & Cuevas, N. (2022). Magnetotelluric investigations of the Kīlauea Volcano, Hawaii. *Journal of Geophysical Research: Solid Earth, 127*(8), e2022JB024418. https://doi.org/10.1029/ 2022JB024418

Ingham, M., & Brown, C. (1998). A magnetotelluric study of the Alpine Fault, New Zealand. *Geophysical Journal International, 135*(2), 542-552. https://doi.org/10.1046/j.1365-246X.1998.00659.x

Junian, W. E., Adilla, R., & Irawati, S. M. (2025). Implementasi algoritma grey wolf optimizer (GWO) untuk pemodelan inversi 1D data magnetotellurik. *Jurnal Geosaintek, 11*(2), 100–261. https://doi.org/10.12962/j25023659.v11i2.2590

Junian, W. E., Grandis, H. (2023). Hybrid Particle Swarm Optimization and Grey Wolf Optimizer Algorithm For Controlled Source Audio- Frequency Magnetotellurics (CSAMT) One- Dimensional Inversion Modelling. Rudarsko-geološko-naftni zbornik, 38 (3), 65-80. https://doi.org/10.17794/rgn.2023.3.6

Junian, W. E., Styawan, Y., Prasetyo, N., Paembonan, A. Y. (2026). Applying the One-to-One-Based Optimizer (OOBO) Algorithm for One-Dimensional Inversion Modeling of Magnetotellurics Data. *Pure Appl. Geophys.* https://doi.org/10.1007/ s00024-026-03998-x

Khatami, M., & Grandis, H. (2023). One-dimensional magnetotelluric (MT) data inversion modeling using convolutional neural network. *IOP Conference Series: Earth and Environmental Science, 1227*, 012023. https://doi.org/10.1088/1755-1315/1227/1/012023

Ladanivskyy, B., Pronenko, V., & Korepanov, V. (2021). Magnetotelluric method and instrumentation for geothermal prospecting. *World Geothermal Congress 2020+1.* Reykjavik, Iceland. https:// www.worldgeothermal.org/pdf/IGAstandard/WGC/2020/13080.pdf

Levy, S., Laloy, E., & Linde, N. (2023). Variational Bayesian inference with complex geostatistical priors using inverse autoregressive flows. *Computers & Geosciences, 171*, 105263. https://doi.org/10.1016/j.cageo.2022.105263

Mekkawi, M. M., Abd-El-Nabi, S. H., Farag, K. S., & Elhamid, M. Y. (2022). Geothermal resources prospecting using magnetotelluric and magnetic methods at Al Ain AlSukhuna-Al Galala Albahariya area, Gulf of Suez, Egypt. *Journal of African Earth Sciences, 190*, 104522.https://doi.org/10.1016/j.jafrearsci.2022.104522

Ojo, A., Xie, J., & Olorunfemi, M. O. (2017). Nonlinear inversion of resistivity sounding data for 1-D earth models using the neighbourhood algorithm. *Journal of African Earth Sciences, 137*, 179-192. https://doi.org/ 10.1016/j.jafrearsci.2017.09.003

Pace, F., Santilano, A., & Godio, A. (2019). Particle swarm optimization of 2D magnetotelluric data. *Geophysics, 84*(3), E125–E141. https://doi.org/10.1190/geo2018-0166.1

Patro, P. K. (2017). Magnetotelluric studies for hydrocarbon and geothermal resources: Examples from the Asian region. *Surveys in Geophysics, 38*, 1005–1041. https://doi.org/ 10.1007/s10712-017-9439-x

Saibi, H., Hireche, A., Ahmad, A., Tsuji, T., & Ali, M. (2026). Comparison of deep learning models for 1D magnetotelluric inversion. *Applied Computing and Geosciences, 29*, 100320. https://doi.org/10.1016/ j.acags.2026.100320

Sambridge, M. (1999a). Geophysical inversion with a neighbourhood algorithm—I. Searching a parameter space. *Geophysical Journal International, 138*(2), 479–494. https://doi.org/10.1046/j.1365246X.1999.0087 6.x

Sambridge, M. (1999b). Geophysical inversion with a neighbourhood algorithm—II. Appraising the ensemble. *Geophysical Journal International, 138*(3), 727–746. https://doi.org/10.1046/j.1365246x.1999.00900 .x

Simeng, P., Xingbing, X., & Lianqun, Z. (2025). Application of the magnetotelluric method in geothermal exploration in Jianshi county, Hubei province, China. *Discover Geosciences, 3*, 70. https://doi.org/10.1007/s44288-025-00181-y

Stoico, V., Dragomir, A. C., & Lago, P. (2025). An empirical study on the performance and energy usage of compiled Python code. *Proceedings of the 29th International Conference on Evaluation and Assessment in Software Engineering (EASE 2025).* Istanbul,Türkiye. https://doi.org/10.1145/3756681.3756972

Sun, X., Zhan, Y., Unsworth, M., Egbert, G., Zhang, H., Chen, X., Zhao, G., Sun, J., Zhao, L., Cui, T., Liu, Z., & Han, J. (2020). 3-D magnetotelluric imaging of the easternmost Kunlun Fault: Insights into strain partitioning and the seismotectonics of the Jiuzhaigou Ms7.0 earthquake. *Journal of Geophysical Research: Solid Earth, 125*(5), e2020JB019731. https://doi.org/ 10.1029/2020JB019731

Syaripudin, A., & Grandis, H. (2001). Inversi Data Magnetotellurik 1-D Mengunakan Metoda Simulated Annealing. *Kontribusi Fisika Indonesia (KFI), 12*(02).

Telford, W. M., Geldart, L. P., & Sheriff, R. E. (1990). *Applied geophysics* (2nd ed.). Cambridge UniversityPress. https://doi.org/10.1017/CBO9781139167932

Unsworth, M. J., Jones, A. G., Wei, W., Marquis, G., Gokarn, S. G., Spratt, J. E., Bedrosian, P., Booker, J., Chen, L., Clarke, G., Li, S., Lin, C., Deng, M., Jin, S., Solon, K., Tan, H., Ledo, J., & Roberts, B. (2005). Crustal rheology of the Himalaya and Southern Tibet inferred from magnetotelluric data. *Nature, 438*, 78-81. https://doi.org/10.1038/nature04154

Wathelet, M. (2008). An improved neighborhood algorithm: Parameter conditions and dynamic scaling. *Geophysical Research Letters, 35*(9),L09301.https://doi.org/10.1029/2008GL 033256

Wu, S., Sun, J., & Chen, J. (2025). Variational inference for geophysical Bayesian inverse problems using normalizing flows: An unsupervised approach to electromagnetic data inversion. *Geophysical Journal International, 242*(3), 1-14. https://doi.org/ 10.1093/gji/ggaf239

Yao, H. (2015). A method for inversion of layered shear wavespeed azimuthal anisotropy from Rayleigh wave dispersion using the Neighborhood Algorithm. *Earthquake Science, 28*, 59–69. https:// doi.org/10.1007 /s11589-014-0108-6

Yoshizawa, K., & Kennett, B. L. (2002). Non-linear waveform inversion for surface waves with a neighbourhood algorithm—application to multimode dispersion measurements. *Geophysical Journal International, 149*(1), 118-133.https://doi.org/10.1046/j.1365246X.20 02.01634.x